Role of Moderately Hydrophobic Chitosan Flocculants in the Removal of Trace Antibiotics from Water and Membrane Fouling Control

Zhen Yang [a], Tianyang Hou [a], Jiangya Ma [c], Bo Yuan [d], Ziqi Tian [e], Weiben Yang [a,*], Nigel J.D. Graham [b,*]

[a] School of Chemistry and Materials Science, Jiangsu Provincial Key Laboratory of Materials Cycling and Pollution Control, Nanjing Normal University, Nanjing, 210023, P.R. China

[b] Department of Civil and Environmental Engineering, Imperial College London, South Kensington Campus, London SW7 2AZ, UK

[c] School of Civil Engineering and Architecture, Anhui University of Technology, Maanshan, Anhui 243002, China

[d] Jiangsu Sinography Testing Co., Ltd., Nanjing 210061, P.R. China

[e] Ningbo Institute of Materials Technology & Engineering, Chinese Academy of Sciences, Ningbo 315000, P.R. China

[*] Corresponding authors.

E-mail addresses: yangzhen@njnu.edu.cn (Z.Y.), 597577871@qq.com (T.H.), majiang_ya@126.com (J.M.), bo.yuan@sino-sut.com (B.Y.), tianziqi@nimte.ac.cn (Z.T.), yangwb007@njnu.edu.cn (W.Y.), n.graham@imperial.ac.uk (N.G.)

Abstract: In this paper we describe the preparation and testing of a new class of chitosan-based flocculants for the treatment of surface waters containing antibiotic compounds. Three forms of moderately hydrophobic chitosan flocculants (MHCs) were prepared by chemically grafting hydrophobic branches with different lengths onto hydrophilic chitosan and these were evaluated by jar tests and a bench-scale continuous flow ultrafiltration (UF) membrane process with coagulation/sedimentation pre-treatment. Tests were conducted using both synthetic and real surface water in which norfloxacin and tylosin were added as representative antibiotics at an initial concentration of 0.1 μg/L. In jar tests, the MHCs achieved similar high removal efficiencies (REs) of turbidity and UV_{254} absorbance, but much higher REs of the two antibiotics (71.7-84.7% and 68.7-76.6% for synthetic and river waters, respectively), compared to several commercial flocculants; the superior performance was attributed to an enhanced hydrophobic interaction and H-bonding between the flocculants and antibiotics. The presence of suspended kaolin particles and humic acid enhanced the antibiotic removal, speculated to be through MHC bridging of the kaolin/ humic acid and antibiotic molecules. In the continuous flow tests involving flocculation/sedimentation-UF for 40 days, an optimal MHC achieved a much greater performance than polyaluminium chloride in terms of the overall removal of antibiotics (RE(norfloxacin) of ~90% and RE(tylosin) of ~80%) and a greatly reduced rate of membrane fouling; the latter resulting from a more porous and looser structure of cake layer, caused by a surface-modification-like effect of residual MHC on the hydrophobic PVDF membrane. The results of this study have shown that MHCs offer a significant advance over the use of existing flocculants for the treatment of surface water.

Keywords: Moderately hydrophobic flocculants; Chitosan; Flocculation;

Ultrafiltration; Antibiotics; Surface water treatment

1. Introduction

The increasing worldwide contamination of surface waters (especially those used for drinking water supplies) caused by micropollutants has been an important challenge for humanity (Schwarzenbach et al. 2006), and continues to be so. One important group of anthropogenic micropollutants are antibiotics, which are of concern owing to possible chronic adverse effects on humans after long-term exposure or through persistent (bio-)accumulation, despite their presence in trace concentrations in surface waters (Petrie et al. 2015, Ying et al. 2017, Bielen et al. 2017). To meet this challenge, effective water treatment technologies are required, either as new or improved existing processes, in order to reduce the concentration of trace antibiotics to levels that pose a minimal risk to the public.

Flocculation (floc generation/development, followed usually by floc settling/flotation) coupled with subsequent ultrafiltration (UF) has been widely studied and found to be an effective, reliable and economical process alternative among many drinking water treatment approaches (Keeley et al. 2016, Su et al. 2017, Ding et al. 2018). In this arrangement, flocculation has an important role in controlling fouling of the UF membrane (Choi and Dempsey 2004, Peleato et al. 2017), while the UF, by virtue of its separation efficiency, compactness, facile automation and small footprint, can remove the remaining, difficult to separate, flocculant-contaminant aggregates, thereby producing an enhanced quality of produced water (Gao et al. 2011). However, conventional flocculation exhibits a poor performance for the removal of water-soluble antibiotics with low molecular weight, since the flocs are unable to bind to the small antibiotic molecules to form coagulation

nuclei at a meso-scale (Melo-Guimaraes et al. 2013, Liu et al. 2019, Wang et al. 2018a). In these circumstances, free (uncoagulated) antibiotic molecules are able to pass through UF membranes (nominal pore size ~ 500kDa MWCO; ~30nm), leading to a poor removal and their presence in treated waters (Cheng et al. 2018). Furthermore, although a large proportion of the contaminants causing membrane fouling can be removed by the flocculation pre-treatment, residual flocculants, either free or within suspended aggregates, are able to act as foulants directly, or facilitate fouling of the UF membrane (Iversen et al. 2009, Liu et al. 2017, Cheng et al. 2017).

In view of the above concerns, one innovative approach, as presented in this study, is the development of new flocculants with a particular structure designed to improve the process performance. This can be achieved by the modification of organic polymers, such as chitosan, which has received considerable attention in the literature previously (Yang et al. 2014). In order to enhance the binding ability towards antibiotics, it is necessary to introduce hydrophobic segments onto the hydrophilic (chitosan) polymer in order to strengthen the hydrophobic association between the flocculant and the antibiotic molecules, thereby promoting the formation of flocculant-contaminant aggregates at meso-scale (Liu et al. 2019, Ren et al. 2017, Du et al. 2018). Furthermore, according to previous studies concerned with the modification of membranes for fouling control (Werber et al. 2016, Rana and Matsuura 2010), the presence of moderately hydrophobic flocculants on the surface of UF membranes, as a residual from upstream flocculation, may mitigate fouling. That is, through hydrophobic association between hydrophobic segments of the flocculants and the membrane matrix, the hydrophilic parts of the flocculants are exposed towards the water phase, giving rise to hydration layers with surface-bound hydrophilic polymer chains, which are desired for inhibition of foulant formation

97 (Kang and Cao 2014). Compared to the conventional approach that involves
98 modification of the membrane during its preparation, which has the shortcomings of
99 peeling/delamination of the coating during the membrane filtration process (Kang and
100 Cao 2014), the surface-modification-like effect of residual (moderately hydrophobic)
101 flocculants can ensure the dynamic stability of the adsorbed layers (with an
102 equilibrium between layers forming and leaching), as residual flocculants are
103 continuously present in the influent to the UF process. To-date, there have been few
104 studies that have considered the interaction between moderately hydrophobic
105 flocculants and antibiotics at trace levels (such as μg/L), or the performance (both
106 contaminant removal and membrane fouling control) of such flocculants in a
107 combined flocculation-UF systems for surface water treatment.

108 In this work, moderately hydrophobic chitosan flocculants (MHCs, in which
109 chitosan (CS) was modified by adding chemically-bonded hydrophobic grafting
110 branches), with different degrees of hydrophobicity, were investigated for the removal
111 of trace antibiotics. Two common antibiotics, norfloxacin (NOR) and tylosin (TYL),
112 with aromatic and macrolides structures, respectively, were selected as target
113 compounds, and their removal by MHCs was evaluated in both synthetic surface
114 water (prepared in the laboratory) and real surface water collected from the Yangtze
115 River. Both jar tests and laboratory-scale continuous-flow flocculation-UF tests were
116 conducted, to quantify and optimize the performance of the flocculants in terms of
117 both water quality improvement (removal of antibiotics), and reduced fouling of the
118 UF membrane. The underlying mechanisms for the enhanced performance were
119 investigated by use of both experimental analyses and computer modelling, in order to
120 better understand the role of MHCs in the flocculation and the combined
121 flocculation-UF processes, and their potential application to practical water treatment.

2. Materials and methods

2.1. Raw water and flocculants

Synthetic surface water was prepared by adding 20 mg of kaolin powder (Sinopharm), 10 mg of humic acid (HA; soluble constituent > 90 wt.%; Aladdin), 1 mmol of $NaHCO_3$ (Sinopharm) and 1 mmol of NaCl (Sinopharm) to 1 L of tap water, which had been left previously to stand for 24 h to ensure the decay of residual chlorine. Real surface water was freshly collected from the Ma'anshan section of the Yangtze River (Caishi Water Factory, Ma'anshan City, Anhui Province) and stored at 4 ^{o}C. Before each batch of experiments, quantities of NOR or TYL antibiotics (Dalian Meilun Biotechnol. Co., Ltd.; their physicochemical properties are listed in the Supporting Information (SI) Table S1; their species distribution curves as a function of pH are given in SI, Fig. S1) were added to the synthetic or real water to obtain a concentration of 0.1 μg/L, and the resulting solution was mixed continuously at ~25 ^{o}C for 24 h to reach equilibrium. Some basic characteristics of the raw water are shown in Table 1.

-Table 1-

The MHCs were prepared according to a two-step "graft-to" method, by chemically-bonding hydrophobic polyacrylpiperidine (PNAPD) branches onto the hydrophilic chitosan backbones, as described in the SI (Text S1 and Fig. S2), and their molecular structure was verified by spectral characterizations, also described in the SI (Text S2 and Fig. S3). Three types of MHCs with different PNAPD branch lengths (by adjusting the molar ratios of chitosan and acrylipiperidine (NAPD), but fixing the molar ratios between chitosan and mercaptoacetic acid) (Hoshino et al. 1998), were obtained and identified as MHC10, MHC20 and MHC30, respectively, as listed in

147 Table 2. Unmodified chitosan (Shandong Aokang Bio-Technol. Co.; deacetylation
148 degree of 86%; viscosity-average-molecular weight of 820 kDa), polyacrylamide
149 (PAM; weight-average-molecular weight 3,000 kDa; Sinopharm) and polyaluminium
150 chloride (PAC; Al_2O_3 content > 28%, Sinopharm) were tested for comparison.
151 -Table 2-
152
153 **2.2. Jar tests**
154 After the pH of equilibrated raw water was adjusted to near-neutral pH (within
155 the range of 6-8), jar tests were carried out using a programmed flocculator
156 (MY3000-6B, Wuhan Meiyu Instrument Co.) at ~25 ^{o}C. A flocculant stock solution of
157 5 g/L was prepared freshly before each jar test. After a known amount of the stock
158 solution was dosed, the flocculation procedure was as follows: 5 min of rapid mixing
159 at 200 rpm, 15 min of slow mixing at 50 rpm, and finally 30 min of floc settling. After
160 settling, samples of the supernatant water were analyzed for turbidity using a
161 WGZ-200 turbidimeter (Shanghai Xinrui Co.). The UV absorbance at 254 nm (UV_{254})
162 of the solution after filtering (0.45-μm filter) was measured by a UV/visible UH5300
163 spectrophotometer (Hitachi). The concentrations of the target antibiotic compounds
164 were determined after solid phase extraction (SPE) by an Ultra Performance Liquid
165 Chromatograph (UPLC) coupled to an electrospray ionization mass spectrometer
166 (ESI-MS). To exclude the complicating influence of antibiotic adsorption onto
167 glassware surfaces, kaolin, and HA, control experiments were conducted for the
168 calibration of removal efficiencies (REs). Every RE was calculated from triplicated
169 parallel tests.
170
171 **2.3. Continuous-flow flocculation-UF tests**

Continuous-flow flocculation-UF tests were performed using a custom-made apparatus as illustrated in Fig. 1. Required flow rates of raw water and flocculant stock solution were pumped into the first 'flocculation' tank for rapid mixing at 200 rpm. The optimal doses of different flocculants were determined from the aforementioned jar tests. The stirring speeds of the following three tanks were 150, 100, and 50 rpm, respectively, to achieve floc growth. The hydraulic residence time (HRT) of each tank was 5 min. After flocculation, the water flowed into an inclined plate settling tank with an HRT of 1 h for floc sedimentation, and then into a submerged UF tank. The UF module consisted of a cluster of hollow fiber UF membranes (Hangzhou Haotian; total (cluster) surface area of 0.025 m^2; pore size of 0.03 μm) made from polyvinylidene fluoride (PVDF). The membrane permeate/produced water was continuously withdrawn by a downstream pump at a stable flux of 20 L/(m^2·h). Intermittent cleaning of the membranes was undertaken after every 30-min of operation, involving a 1-min period of backwash (at 0.66 L/(m^2·min)) and accompanying air scour (2.5 L/min), as used elsewhere (Yu et al. 2015). In addition, the membrane was physically cleaned using a sponge at day 13 and 26. The trans-membrane pressure (TMP) was continuously monitored during the whole period of operation.

-Fig. 1-

2.4. Other characterizations and analyses

The zeta potential (ZP) of water samples, as well as size distribution of MHCs in water, was measured by a Zetasizer (Malvern Nano-Z), and contact angles (CA) of flocculants were determined using a telescopic goniometer (Rame-Hart-100). Molecular dynamics (MD) simulation, in which one PNAPD chain containing the

same length as that of the branches in the MHC10, MHC20 or MHC30 flocculants was simulated in 500 H_2O molecules, was performed in Materials Studio software, based on Consistent Valence Force Field (CVFF) (Mochizuki et al. 2016), in order to express the molecular chain structure in water. Correlation analyses for the RE(turbidity), RE(UV_{254}) and RE(antibiotics) were carried out using the SPSS Statistics software (IBM). Density functional theory (DFT) calculations of geometries and binding energies (BEs) of flocculant-antibiotic complexes were performed using the Gaussian 09 software at the M06-2x/6-31+G(d) level. Images showing the microscopic morphologies of UF membranes after use were captured by scanning electron microscopy (SEM; JEOL JSM-5610LV).

3. Results and discussion

3.1. Surface charge property and hydrophilicity/hydrophobicity of MHCs

The surface charge properties and hydrophilicity/hydrophobicity of the MHCs represent two important intrinsic characteristics affecting their water treatment performance.

ZP-pH curves of CS and MHCs are plotted in Fig. 2a. These show that all of the flocculants had positive surface charges over the near-neutral pH range of raw water (pH 6-8), partly because of the protonated primary amino groups on the CS backbones. In addition, it was evident that the ZP of the MHCs became more positive with the increase of the PNAPD branch lengths. The greater cationic nature of the MHCs was believed to be helpful for achieving charge neutralization in the flocculation of the negatively charged kaolin particles and HA colloids at near-neutral pH conditions (Yang et al. 2016). However, charge neutralization might not be a factor in the binding of the target antibiotics, given that neither compound has any significant proportion of

222 anionic species in the near-neutral pH range, as indicated in the SI (Fig. S1).

223 -Fig. 2-

224 The variation of contact angle (CA) as a function of *N* (average number of
225 repeated units in one PNAPD branch) is shown in Fig. 2b (black line) (images for CA
226 determination provided in SI, Fig. S4). Generally, a larger contact angle indicates that
227 surfaces of materials are more hydrophobic and less hydrophilic. Fig. 2b shows that
228 CAs of MHCs increase with the increase of *N*, indicating that MHCs with longer
229 PNAPD branches are more hydrophobic and less hydrophilic than those with shorter
230 branches. MD simulation results, as illustrated in the SI, Fig. S5, supported the above
231 findings, since the arrangement of hydrophobic piperidine rings is more ordered for
232 PNAPD chains with greater *N*, owing to the stronger intramolecular hydrophobic
233 association. Despite this, the average length of one NAPD repeated unit in PNAPD
234 branches (length of NAPD unit = length of PNAPD branch / *N*, where the length of
235 PNAPD branch is obtained from MD simulation results shown in SI, Fig. S5) is
236 shorter as *N* increases, as depicted by the red line in Fig. 2b. Shorter NAPD length
237 means less space for one NAPD unit to interact with other molecules (such as
238 antibiotics). When one NAPD unit interacts with a large antibiotic molecule, more
239 adjacent NAPD units are likely to be covered by the antibiotic molecule, and therefore
240 the utilization efficiency of NAPD units for interaction with antibiotics will decrease.
241 To sum up, longer PNAPD branches makes MHCs more hydrophobic, but correspond
242 to a lower utilization efficiency of NAPD units. These counterbalancing effects will
243 be discussed further concerning the effect of PNAPD branch length on treatment
244 performance (section 3.2.2).

245

246 **3.2. Jar tests using synthetic water**

The treatment performance of the MHCs in jar tests using the synthetic contaminated water was evaluated and the results are shown in Fig. 3. A summary of the optimal dosages ($dosage_{opt}$) and corresponding highest REs for different water parameters is provided in the SI, Tables S2 and S3. The highest REs reached ~95% (~1 NTU of treated water) for turbidity, ~90% (~0.03 $Abs.cm^{-1}$ of treated water) for UV_{254}, and ~80% for the antibiotics, indicating the excellent performance of MHCs in the treatment of the synthetic surface water. By comparison, when commercial flocculants (PAC, PAM and CS) were employed (Fig. 4), despite their effectiveness for turbidity and UV_{254} removal, all commercial flocculants showed poor removal of antibiotics (REs≤40%). Among the three commercial flocculants, PAC displayed the highest RE(turbidity) (~95%) and RE(UV_{254}) (~90%) values, which were similar to those achieved by MHCs; however, the $dosage_{opt}$ of PAC (~20 mg/L) was much higher than those of MHCs. Various factors were found to affect the treatment performance of the MHCs, namely the pH, flocculant dosage, PNAPD branch length, antibiotic type, the presence of kaolin and HA, and these were analyzed in detail, and are discussed as follows.

-Fig. 3-

-Fig. 4-

3.2.1. Effects of pH and flocculant dosage

In the near-neutral pH range of surface water (6-8), pH did not exert a notable influence on the treatment performance as illustrated in Fig. 3, although it was found that the performance at pH 6 or 7 was slightly greater than at pH 8 for all three parameters in most situations (summary results shown in SI, Tables S2 and S3). For the major contaminants in water (negatively charged kaolin particles and HA), the

slight decline of REs at pH 8 could be explained by weaker charge effects corresponding to the lower cationic ZPs of the flocculants at pH 8 (Fig. 2a). The significance of charge interaction in the flocculation was also indicated by the influence of flocculant dosage, as all RE – dosage profiles in Fig. 3 demonstrated an "up-peak-down" trend (Wang et al. 2018b). At low, sub-optimal dose, the positively charged flocculant can decrease the absolute values of ZPs (|ZP|) (examples of dosing MHC20 into kaolin and HA solution are shown in SI, Fig. S6), as well the stability, of negatively charged kaolin particles and HA through charge attraction between the flocculants and the contaminants, promoting their aggregation and sedimentation. At the optimal flocculant dose (10-12 mg/L), |ZP| values of kaolin and HA are close to zero, indicating the lowest stability of both contaminants, which agrees well with the peak RE values in Fig. 3. At flocculant doses greater than the optimal dose, excessive flocculants are adsorbed onto contaminant particles and increase their |ZP| values again (SI, Fig. S6), and therefore re-stabilization occurs due to electrostatic repulsion among positively charged particles, generating the reduction in treatment performance. However, as mentioned previously, charge effects by the flocculants were not the dominant effect for the removal of the antibiotics, as these were only weakly dissociated (anionic) at the test pH conditions (≤ 8) (SI, Fig. S1). Instead, the reduction in the REs(antibiotic) at flocculant doses above the optimal, and at pH 8, might be related to beneficial effects from the presence of kaolin and HA in solution, which will be discussed later.

3.2.2. Effect of PNAPD branch length

The jar test results for the NOR- and TYL- synthetic contaminated waters, summarized in the SI, Tables S2 and S3, showed an increase in the REs(antibiotic)

297 with increasing branch length from MHC10 to MHC20, but no further increase from
298 MHC20 to MHC30. The improvement from MHC10 to MHC20 might be explained
299 by two factors. Firstly, compared to MHC10, MHC20 with a longer PNAPD branch
300 has a larger CA value (Fig. 2b), implying that MHC20 is more hydrophobic and less
301 hydrophilic than MHC10. This is beneficial to the attachment and incorporation of the
302 antibiotic compounds into floc aggregates *via* hydrophobic association. Secondly, the
303 higher cationic charge (ZP) of the MHC20 (Fig. 2a) can provide an enhanced charge
304 interaction with the negatively charged kaolin and HA, which could promote
305 antibiotic removal by enhanced separation of flocs (containing antibiotic compounds
306 associated with the MHC, kaolin and HA). With regard to the similar performance by
307 MHC20 and MHC30, although the degree of hydrophobicity and ZP was greater for
308 MHC30, the utilization efficiency of NAPD units for interaction with antibiotics
309 decreased as discussed previously in Section 3.1. The greater hydrophobicity also has
310 the effect of reducing the dispersibility of the flocculant during the flocculation
311 reaction, which is confirmed by the notably increased size of MHC30 compared to
312 MHC20 in water (size distribution shown in SI, Fig. S7). Thus, there appeared to be
313 no clear advantage with the use of the higher branch length flocculant (MHC30), and
314 so from an economic standpoint MHC20 represents the optimal flocculant.
315
316 **3.2.3. Effect of antibiotic type**
317 NOR and TYL were used in this work to represent to two different
318 commonly-detected antibiotics in surface water. It was evident from comparison of
319 the compound removal (RE(NOR) values in SI, Table S2 and RE(TYL) values in SI,
320 Table S3) that the optimal REs(NOR) were slightly greater than the corresponding
321 REs(TYL). This indicated that NOR was easier to separate by flocculation than TYL

using MCHs. DFT computations were performed to calculate the BEs between the main groups (repeated NAPD unit) of the MCH and the antibiotics (SI, Fig. S8). According to the optimized geometries of the NAPD-antibiotic complexes, H-bonding and hydrophobic association were both dominant interactions in the flocculation of both antibiotics. As the BE for the NOR-antibiotic was larger than that for the TYL-antibiotic, it was concluded that the stronger binding ability of PNAPD towards NOR led to its greater REs.

3.2.4. Effects of kaolin and HA in solution

Correlations of RE(turbidity)-RE(antibiotic) and RE(UV_{254})-RE(antibiotic) were determined and these are given in the SI, Tables S4 and S5, and based on the results illustrated in Fig. 3. The removal of both antibiotics was found to correlate highly with that of turbidity and UV_{254}. The high correlations indicated that suspended kaolin particles and HA colloids exerted significant enhancement effects on the removal of antibiotics, as the removal of antibiotics was poor, without clear floc formation, when neither kaolin nor HA was present. However, for the same two antibiotic-contaminated synthetic waters, containing the same amounts of kaolin and HA, the enhancement effects were much weaker when commercial flocculants, PAC, PAM and CS, were employed (Fig. 4): although the REs(turbidity) and REs(UV_{254}) for the commercial flocculants reached comparatively high values, the RE(antibiotic) were at a low level. Hence, the enhancement effects evident in Fig. 3 were mainly ascribed to the role of the MHCs, rather than kaolin or HA itself. That is, MCHs effectively bridged the kaolin (or HA) with the antibiotics in the process of flocculation, with the hydrophobic PNAPD branches binding the antibiotic molecules through hydrophobic association and H-bonding as discussed above in section 3.2.3;

the positively charged hydrophilic CS chains were anchored onto the negatively surface charged kaolin particles or HA colloids. Such anchoring interaction can be explained from a theoretical perspective, as follows: within MHC molecules, the N atoms with sp^3 hybrid orbitals in the amino groups on CS chains are more easily protonated than those with sp^2 hybrid orbitals in the amide groups on PNAPD branches; therefore, CS chains, instead of the near-neutral PNAPD branches, contribute the major part of the positive charges of MHC, and are more inclined to anchor onto the negatively charged kaolin or HA. ZP distribution curves of kaolin suspension and HA solution with the addition of different MHC20 dosages (SI, Fig. S9) also provide experimental evidence to demonstrate the anchoring interaction: (1) ZP distribution curves of kaolin (or HA) always remain unimodal without the original peak of MHC20, indicating that the flocculant is tightly bound with kaolin (or HA); (2) MHC20 itself has a high ZP peak value (~20 mV), since its amino groups extend outwards while near-neutral PNAPD branches stretch inward through hydrophobic association. However, after binding onto kaolin (or HA), the peak values of the ZP distribution curves, even at a high MHC20 dosage (16 mg/L), are only slightly greater than zero but much lower than 20 mV. This indicates that near-neutral PNAPD branches of the bound MHC20 extend outward, whereas CS chains with positive charges face inward and participate in the anchoring interaction with kaolin or HA.

3.3. Jar tests using Yangtze River water

Further jar tests were undertaken showing the flocculation performance of the MHCs using NOR or TYL spiked into samples of Yangtze River water (Fig. 5). A summary of the $dosage_{opt}$ and corresponding REs for the three pH conditions are listed in the SI (Tables S6 and S7). The highest REs, reaching ~95% (~1 NTU in

372 treated water) for turbidity, ~70% (~0.03 Abs.cm^{-1} in treated water) for UV_{254}, ~75%
373 for the antibiotics, demonstrated that the MHCs were effective in the treatment of the
374 real surface water, in agreement generally with the performance observed with the
375 synthetic water. However, owing to the differences in the water quality between the
376 synthetic and real waters, there were some differences in the flocculation performance
377 of both waters. In particular, the optimal MHC dosages ($dosage_{opt}$) for the Yangtze
378 River water (2-6 mg/L) were significantly lower than those for the synthetic water
379 (10-12 mg/L). The Yangtze River water (dissolved organic carbon (DOC) of 4.80
380 mg/L) had a lower concentration of natural organic matter (NOM) than the synthetic
381 water (DOC of 7.63 mg/L), and therefore, less flocculant was consumed by NOM for
382 electrostatic attraction. In addition, the organic matter (HA) in the synthetic water
383 (>90% of soluble constituent; specific UV absorbance (SUVA) of 4.26 L/(mg.m)) was
384 markedly different from the NOM in the real surface water (SUVA of 2.42 L/(mg.m)),
385 implying a higher proportion of aromatic DOC components in the synthetic water,
386 which would also heighten the flocculation difficulty as flocculant MHC itself is
387 mainly composed of saturated carbon. Hence, the synthetic water with a higher
388 proportion of aromatic DOC components also contributed to the higher flocculant
389 dosage required than the real surface water. Both aspects (NOM quantity and
390 composition) are believed to explain the difference in the optimal flocculant dose for
391 the two types of test water. Apart from the influence of NOM content, the effects of
392 flocculation pH and PNAPD branch length on treatment performance were similar to
393 those found with the synthetic water. As found with the synthetic water, MHC20 was
394 also the best flocculant among the three MHCs for the river water. Also as found with
395 the synthetic water, the beneficial effect of coexisting suspended particles and NOM
396 in the river water, on antibiotic removal, was indicated by the high correlations of the

MHC20 treatment (summarized in the SI, Tables S8 and S9).

-Fig. 5-

3.4. Continuous-flow flocculation-UF tests

As MHC20 was found to be the optimal flocculant in the jar tests for both the synthetic and Yangtze River waters, it was employed for the subsequent continuous-flow flocculation-UF tests. Among the three commercial flocculants (PAC, PAM, and CS) used in the jar tests, PAC displayed the best performance for the removal of turbidity and UV_{254}, and was therefore used for comparison in the continuous-flow flocculation-UF tests. In both cases (MHC20 and PAC), synthetic contaminated water with the target antibiotics was used as the test solution.

3.4.1. Produced water quality

Produced water qualities after the sedimentation and UF treatment of the NOR- and TYL-contaminated synthetic waters are shown in Fig. 6 (a, b, d and e). In terms of the removal of turbidity and UV_{254}, both flocculants exhibited a high degree of treatment, reaching a removal of ~95% or greater in the initial period of several days and then subsequently. Following the flocculation-sedimentation stages, the UF stage further increased the RE(turbidity) and RE(UV_{254}) in both the MHC20 and PAC systems, due to the filtration of remaining kaolin particles and humic acid colloids. The main difference between the two systems was in the removal of the antibiotic compounds. In this respect, the MHC20 treatment system showed a notable superiority over the PAC system, with the average RE(NOR) and RE(TYL) for the stable treatment period (10-40 days) equal to 90.8% and 80.4%, respectively, for the MHC, compared to 71.2% and 52.0%, respectively, for the PAC. The total RE(antibiotic) in the continuous process could be divided into the

flocculation-sedimentation part (part A), and the UF membrane part (part B); the latter was achieved via separation of residual flocs (with incorporated antibiotics) and direct adsorption on the hydrophobic PVDF surface. Calculations using the data for the stable treatment period (10-40 days) of the MHC systems (Fig. 6 (b and e)) showed that part A's contributions to the total RE(antibiotic) were 79.6% for NOR and 69.0% for TYL, respectively; whereas part B's contributions were much smaller, only 11.2% for NOR and 11.4% for TYL, respectively. Therefore, it was evident that the flocculation-sedimentation stages were mainly responsible for the overall antibiotic removal performance.

-Fig. 6-

In view of the growing concerns about the toxicity of chemicals used in water treatment, as well as disinfection-by-product (DBP) formation, the possible implications of residual MHC20 in the treated water is discussed as follows. Theoretically, the overall toxicity risk of MHC20 itself is low according to information in the literature: CS is a natural biopolymer with good biocompatibility and no toxicity; the N-alkyl-substituted polyacrylamide has been widely applied as an in-vivo drug delivery vehicle, and is biocompatible with low toxicity (Phillips and Gibson. 2015); the toxicity can be further reduced by conjugating poly(N-alkyl-substituted acrylamide) with natural polymers (Kaur et al. 2015). Residual MHC20 concentrations in the treated water were also measured using a DOC-based method, after small organic molecules were separated from MHC20 in the water samples using 100 kDa molecular weight cutoff (considering the molecular size distribution of MHC20 shown in SI Fig. S7) flat sheet UF membranes. The concentration of MHC20 after flocculation-sedimentation was ~0.40 mg/L; despite this, the residual concentration in the final effluent after the UF membrane (pore size

of 0.03 μm) in the continuous treatment process was negligible (lower than the lower detection limit), and this result was consistent with the size distribution (SI, Fig. S7). Therefore, the likelihood of negative impacts from the presence of residual flocculant in the final treated water is considered to be very slight.

3.4.2. TMP variation

The temporal development of TMP over the 40 days of operation for the two systems is shown in Fig. 6 (c and f). The results indicate that the TMP of the PAC system increased much more rapidly than that of the MHC20 system. In the initial period of 13 days, the TMP of the PAC system increased by 3-4 kPa, compared to only ~2 kPa for the MHC20 system. The first sponge washing on day 13 was effective in restoring the TMP to nearly the original values for both of the PAC and MHC20 systems (2 kPa). However, after the second washing on day 26, the TMP for the PAC system was much greater (9.0 and 9.8 kPa for NOR- and TYL- contaminated water, respectively) than the original clean membrane value, indicating substantial irreversible fouling. By contrast, irreversible fouling for the MHC20 system is notably reduced, with TMP of 3.7 and 3.9 kPa for NOR- and TYL- contaminated water, respectively. Thus, the development of irreversible fouling, associated with a high attachment strength between foulants and membrane surface, was more difficult for the MHC20 case. At the end of the experimental period at day 40, for both antibiotic-contaminated waters, the TMP of the MHC20 system remained lower than 6 kPa, while for the PAC system it had reached 14 kPa. These results showed clearly that the flocculation pretreatment using MHC20 had greatly mitigated membrane fouling compared to PAC; this has the potential benefits in practice of lowering chemical cleaning frequency and prolonging membrane life. As indicated previously

by both the experimental studies and theoretical analyses, the PNAPD branches of the MCHs provided hydrophobic-type sites for interactions with solutes and surfaces, which were complementary to the hydrophilic nature of the CS backbone. The role of the MCH20 in fouling inhibition was thus attributed to the surface-modification-like effect of residual MHC20 (in soluble form or associated with suspended flocs in the UF influent water after sedimentation) on the hydrophobic PVDF membrane: this could occur by PNAPD branches being anchored onto the PVDF surface and CS chains forming a hydrophilic layer outside the surface, and providing a steric repulsive barrier with resistance to fouling.

3.4.3. SEM images

The cake layer that forms on the membrane during operation is one of the determinants of membrane fouling. SEM images of the membrane after 40 days of operation are presented in Fig. 7 (cake layers) and SI, Fig. S10 (membrane surface after sponge washing). For the tests using both antibiotic-contaminated waters, despite no distinct difference of the PVDF membrane surface after washing the cake layers (SI, Fig. S10), there were clear differences in the cake layer between the PAC and MHC20 systems (Fig. 7): the cake layers of the PAC system were much more compact and covered much of the surface of the membrane. In contrast, the cake layers of the MHC20 system, though slightly thicker than those of the PAC system (the average cake layer thickness were analyzed using Image ImagePro® Plus 6.0; detailed methods were given in SI, Text S4), had a looser structure with more large pores. Such porous and loose morphology possibly resulted from the steric repulsive barrier effect of the MHC20, as mentioned previously (the hydration layer, caused by hydrophilic CS chains binding with water molecules, acting as a steric repulsive

barrier with resistance to fouling, and making the cake layer easily broken) (Chen et al. 2011, Werber et al. 2016), and was believed to have a much lower hydraulic resistance (Sun et al. 2017, Ma et al. 2018), as indicated by the results of the TMP development (Fig. 6 (c and f)).

-Fig. 7-

4. Conclusions

Novel MHCs with controlled hydrophobicity (MHC20) were found to be highly effective in the removal of trace antibiotics (initial concentration of 0.1 μg/L) and mitigating membrane fouling in the combined flocculation-UF treatment of surface water. In jar flocculation tests, as well as achieving high REs for turbidity and UV_{254} absorbing substances, the REs of the two target antibiotics were 71.7-84.7% and 68.7-76.6% for the synthetic and Yangtze River waters, respectively, under the corresponding optimal MHC20 dosages. In continuous operation of the combined flocculation-UF process, a higher permeate water quality (RE(norfloxacin) of ~88% and RE(tylosin) of ~80%) and better fouling control performance (TMP increase of 4 kPa after 40-day operation at a flux of 0.33 L/(m^2·min)) were achieved when MHC20 was used as the flocculant, compared to PAC. The greater performance of MHC20 in the removal of trace antibiotics resulted from an enhanced hydrophobic interaction and H-bonding between the flocculant and antibiotic compounds; in addition, through charge attraction to kaolin or HA, the MHC20 facilitated the bridging of the kaolin (or HA) and antibiotics, which demonstrated the enhancement of antibiotic removal by the presence of coexisting kaolin and HA concentrations. Regarding the beneficial role of MHC20 in reducing membrane fouling, this was attributed to a surface-modification-like effect of residual flocculant on the PVDF UF membrane, in

which hydrophobic PNAPD branches were anchored onto the PVDF surface and CS chains formed hydrophilic steric repulsive barriers outside. Such barriers not only inhibited fouling formation, but also engendered a porous and loosely structured cake layer, with a reduced hydraulic resistance.

Acknowledgements

The authors gratefully acknowledge the National Natural Science Foundation of China (51978341, 51608275), the Project for Comprehensive Management of Water Environment of Tai Lake of Jiangsu Province (TH2018201), National Major Project of Science and Technology Ministry of China (2017ZX07202-004), Visiting Scholar Project of China Scholarship Council, Jiangsu Collaborative Innovation Centre of Biomedical Functional Materials, a project funded by the Priority Academic Program Development (PAPD) of Jiangsu Higher Education Institutions, and the Scientific Computing Centre of NNU.

References

Bielen, A., Šimatović, A., Kosić-Vukšić, J., Senta, I., Ahel, M., Babić, S., Jurina, T., González Plaza, J.J., Milaković, M. and Udiković-Kolić, N. (2017) Negative environmental impacts of antibiotic-contaminated effluents from pharmaceutical industries. Water Research 126, 79-87.

Chen, W., Su, Y., Peng, J., Dong, Y., Zhao, X. and Jiang, Z. (2011) Engineering a robust, versatile amphiphilic membrane surface through forced surface segregation for ultralow flux-decline. Advanced Functional Materials 21(1), 191-198.

Cheng, X., Liang, H., Ding, A., Zhu, X., Tang, X., Gan, Z., Xing, J., Wu, D. and Li, G. (2017) Application of Fe(II)/peroxymonosulfate for improving ultrafiltration membrane performance in surface water treatment: Comparison with coagulation and ozonation. Water Research 124, 298-307.

Cheng, X., Wu, D., Liang, H., Zhu, X., Tang, X., Gan, Z., Xing, J., Luo, X. and Li, G. (2018)

549 Effect of sulfate radical-based oxidation pretreatments for mitigating ceramic UF membrane
550 fouling caused by algal extracellular organic matter. Water Research 145, 39-49.
551 Choi, K.Y.J. and Dempsey, B.A. (2004) In-line coagulation with low-pressure membrane filtration.
552 Water Research 38(19), 4271-4281.
553 Ding, Q., Yamamura, H., Yonekawa, H., Aoki, N., Murata, N., Hafuka, A. and Watanabe, Y. (2018)
554 Differences in behaviour of three biopolymer constituents in coagulation with polyaluminium
555 chloride: Implications for the optimisation of a coagulation-membrane filtration process. Water
556 Research 133, 255-263.
557 Du, H., Yang, Z., Tian, Z., Huang, M., Yang, W., Zhang, L. and Li, A. (2018) Enhanced removal of
558 trace antibiotics from turbid water in the coexistence of natural organic matters using
559 phenylalanine-modified-chitosan flocculants: Effect of flocculants' molecular architectures.
560 Chemical Engineering Journal 333, 310-319.
561 Gao, W., Liang, H., Ma, J., Han, M., Chen, Z.L., Han, Z.S. and Li, G.B. (2011) Membrane fouling
562 control in ultrafiltration technology for drinking water production: A review. Desalination
563 272(1-3), 1-8.
564 Hoshino, K., Taniguchi, M., Kitao, T., Morohashi, S. and Sasakura, T. (1998) Preparation of a new
565 thermo-responsive adsorbent with maltose as a ligand and its application to affinity
566 precipitation. Biotechnology and bioengineering 60(5), 568-579.
567 Iversen, V., Mehrez, R., Horng, R.Y., Chen, C.H., Meng, F., Drews, A., Lesjean, B., Ernst, M.,
568 Jekel, M. and Kraume, M. (2009) Fouling mitigation through flocculants and adsorbents
569 addition in membrane bioreactors: Comparing lab and pilot studies. Journal of Membrane
570 Science 345(1-2), 21-30.
571 Kang, G.D. and Cao, Y.M. (2014) Application and modification of poly(vinylidene fluoride)
572 (PVDF) membranes - A review. Journal of Membrane Science 463, 145-165.
573 Kaur, S., Prasad, C., Balakrishnan, B. and Banerjee, R., 2015. Trigger responsive polymeric
574 nanocarriers for cancer therapy. Biomaterials Science 3 (7), 955-987.
575 Keeley, J., Jarvis, P., Smith, A.D. and Judd, S.J. (2016) Coagulant recovery and reuse for drinking
576 water treatment. Water Research 88, 502-509.
577 Liu, J., Cheng, S., Cao, N., Geng, C., He, C., Shi, Q., Xu, C., Ni, J., DuChanois, R.M., Elimelech,

578 M. and Zhao, H. (2019) Actinia-like multifunctional nanocoagulant for single-step removal of
579 water contaminants. Nature Nanotechnology 14(1), 64-71.
580 Liu, T., Lian, Y., Graham, N., Yu, W., Rooney, D. and Sun, K. (2017) Application of
581 polyacrylamide flocculation with and without alum coagulation for mitigating ultrafiltration
582 membrane fouling: Role of floc structure and bacterial activity. Chemical Engineering Journal
583 307, 41-48.
584 Ma, B., Qi, J., Wang, X., Ma, M., Miao, S., Li, W., Liu, R., Liu, H. and Qu, J. (2018) Moderate
585 $KMnO_4$-Fe(II) pre-oxidation for alleviating ultrafiltration membrane fouling by algae during
586 drinking water treatment. Water Research 142, 96-104.
587 Melo-Guimaraes, A., Torner-Morales, F.J., Duran-Alvarez, J.C. and Jimenez-Cisneros, B.E. (2013)
588 Removal and fate of emerging contaminants combining biological, flocculation and membrane
589 treatments. Water Science and Technology 67(4), 877-885.
590 Mochizuki, K., Sumi, T. and Koga, K. (2016) Driving forces for the pressure-induced aggregation
591 of poly(N-isopropylacrylamide) in water. Physical Chemistry Chemical Physics 18(6),
592 4697-4703.
593 Peleato, N.M., Legge, R.L. and Andrews, R.C. (2017) Characterization of UF foulants and fouling
594 mechanisms when applying low in-line coagulant pre-treatment. Water Research 126, 1-11.
595 Petrie, B., Barden, R. and Kasprzyk-Hordern, B. (2015) A review on emerging contaminants in
596 wastewaters and the environment: Current knowledge, understudied areas and
597 recommendations for future monitoring. Water Research 72, 3-27.
598 Phillips, D.J. and Gibson, M.I., 2015. Towards being genuinely smart: ‘iso-thermally-responsive’
599 polymers as versatile, programmable, scaffolds for biologically-adaptable materials. Polymer
600 Chemistry 6 (7), 1033-1043.
601 Rana, D. and Matsuura, T. (2010) Surface modifications for antifouling membranes. Chemical
602 reviews 110(4), 2448-2471.
603 Ren, K., Du, H., Yang, Z., Tian, Z., Zhang, X., Yang, W. and Chen, J. (2017) Separation and
604 sequential recovery of tetracycline and Cu(II) from water using reusable thermoresponsive
605 chitosan-based flocculant. ACS Applied Materials & Interfaces 9(11), 10266-10275.
606 Schwarzenbach, R., Escher, B., Fenner, K., Hofstetter, T., Johnson, C., Von Gunten, U. and Wehrli,

607 B. (2006) The challenge of micropollutants in aquatic systems. Science 313(25), 1072-1077.
608 Su, Z., Liu, T., Yu, W., Li, X. and Graham, N.J.D. (2017) Coagulation of surface water:
609 Observations on the significance of biopolymers. Water Research 126, 144-152.
610 Sun, J., Hu, C., Tong, T., Zhao, K., Qu, J., Liu, H. and Elimelech, M. (2017) Performance and
611 mechanisms of ultrafiltration membrane fouling mitigation by coupling coagulation and
612 applied electric field in a novel electrocoagulation membrane reactor. Environmental Science
613 & Technology 51(15), 8544-8551.
614 Wang, N., Xu, Z., Xu, W., Xu, J., Chen, Y. and Zhang, M. (2018a) Comparison of coagulation and
615 magnetic chitosan nanoparticle adsorption on the removals of organic compound and
616 coexisting humic acid: A case study with salicylic acid. Chemical Engineering Journal 347,
617 514-524.
618 Wang, X., Gan, Y., Guo, S., Ma, X., Xu, M. and Zhang, S. (2018b) Advantages of titanium xerogel
619 over titanium tetrachloride and polytitanium tetrachloride in coagulation: A mechanism
620 analysis. Water Research 132, 350-360.
621 Werber, J.R., Osuji, C.O. and Elimelech, M. (2016) Materials for next-generation desalination and
622 water purification membranes. Nature Reviews Materials 1(5), 16018.
623 Yang, Z., Li, H., Yan, H., Wu, H., Yang, H., Wu, Q., Li, H., Li, A. and Cheng, R. (2014)
624 Development of a novel chitosan-based flocculant with high flocculation performance, low
625 toxicity and good floc properties. Journal of Hazardous Materials 276, 480-488.
626 Yang, Z., Ren, K., Guibal, E., Jia, S., Shen, J., Zhang, X. and Yang, W. (2016) Removal of trace
627 nonylphenol from water in the coexistence of suspended inorganic particles and NOMs by
628 using a cellulose-based flocculant. Chemosphere 161, 482-490.
629 Ying, G.G., He, L.Y., Ying, A.J., Zhang, Q.Q., Liu, Y.S. and Zhao, J.L. (2017) China must reduce
630 its antibiotic use. Environmental Science & Technology 51(3), 1072-1073.
631 Yu, W.Z., Graham, N., Yang, Y.J., Zhou, Z.Q. and Campos, L.C. (2015) Effect of sludge retention
632 on UF membrane fouling: The significance of sludge crystallization and EPS increase. Water
633 Research 83, 319-328.

634

Captions

Table 1. Water quality parameters of the raw and treated water.

Table 2. Characteristic parameters of MHC flocculants.

Fig. 1. Custom-made continuous-flow flocculation-UF apparatus.

Fig. 2. (a) Zeta potential (ZP) variation with pH for CS and MHCs; (b) Variation of contact angle and average length per repeated NAPD unit of different flocculants (average number of repeated units in one PNAPD branch: MCH10: 7; MHC20: 16; MHC30: 24).

Fig. 3. Performance of MHCs for the treatment of synthetic water in jar flocculation tests.

Fig. 4. Flocculation performance of PAC, PAM and CS for treatment of (a-c) NOR- and (d-f) TYL-contaminated synthetic water.

Fig. 5. Performance of MHCs for the treatment of Yangtze River water in jar flocculation tests.

Fig. 6. Performance of MHC20 and PAC for the treatment of (a, b) NOR- and (d, e) TYL-contaminated synthetic water in continuous-flow flocculation-UF tests (water qualities after treatment by (a and d) PAC and (b and e) MHC20; (c and f) variation of TMP with time).

Fig. 7. SEM images of membrane surface after 40 days of flocculation-UF operation for (a and b) NOR- and (c and d) TYL-contaminated water ((a and c) PAC and (b and d) MHC20 were used as flocculants, respectively; Insert figures: Cross-section of cake layers).

Table 1
Click here to download Table: Table 1.docx

Table 1. Water quality parameters of the raw and treated water.

	Synthetic water	Yangtze River water [a]	Treated water in jar tests		Treated water in continuous-flow flocculation-UF tests	
			Treated synthetic water [b]	Treated Yangtze River water [b]	Effluent after flocculation-sedimentation	Effluent after UF
Turbidity (NTU)	23.8	21.0	0.48-1.67	0.63-1.47	1.85±0.78	0.65±0.47
UV_{254} ($Abs.cm^{-1}$)	0.325	0.116	0.017-0.049	0.036-0.041	0.037±0.011	0.027±0.012
Antibiotic (ng/L) [c]	100	100	15.3-18.0(NOR) 21.1-28.3(TYL)	26.8-30.9(NOR) 23.4-31.3(TYL)	23.0±7.0(NOR) 31.9±4.3(TYL)	11.8±7.6(NOR) 20.3±4.3(TYL)

[a] Raw Yangtze River water collected from Caishi Water Factory, Ma'anshan City, Anhui province

[b] Treated water under the corresponding optimal flocculation conditions using MHC20 as the flocculant

[c] Antibiotic concentration (NOR or TYL) artificially added into raw water

Table 2. Characteristic parameters of MHC flocculants.

Sample	n(CS):n(NAPD) in raw materials	Average number of repeated NAPD units in one PNAPD branch [a]	Grafting ratio [b] (wt.%)
CS	-	0	0
MHC10	1:10	7.1	375
MHC20	1:20	16.7	882
MHC30	1:30	24.5	1294

[a] determined by acid-base titration, detailed method provided in SI, Table S3.

[b] determined by elemental analysis

Figure 1

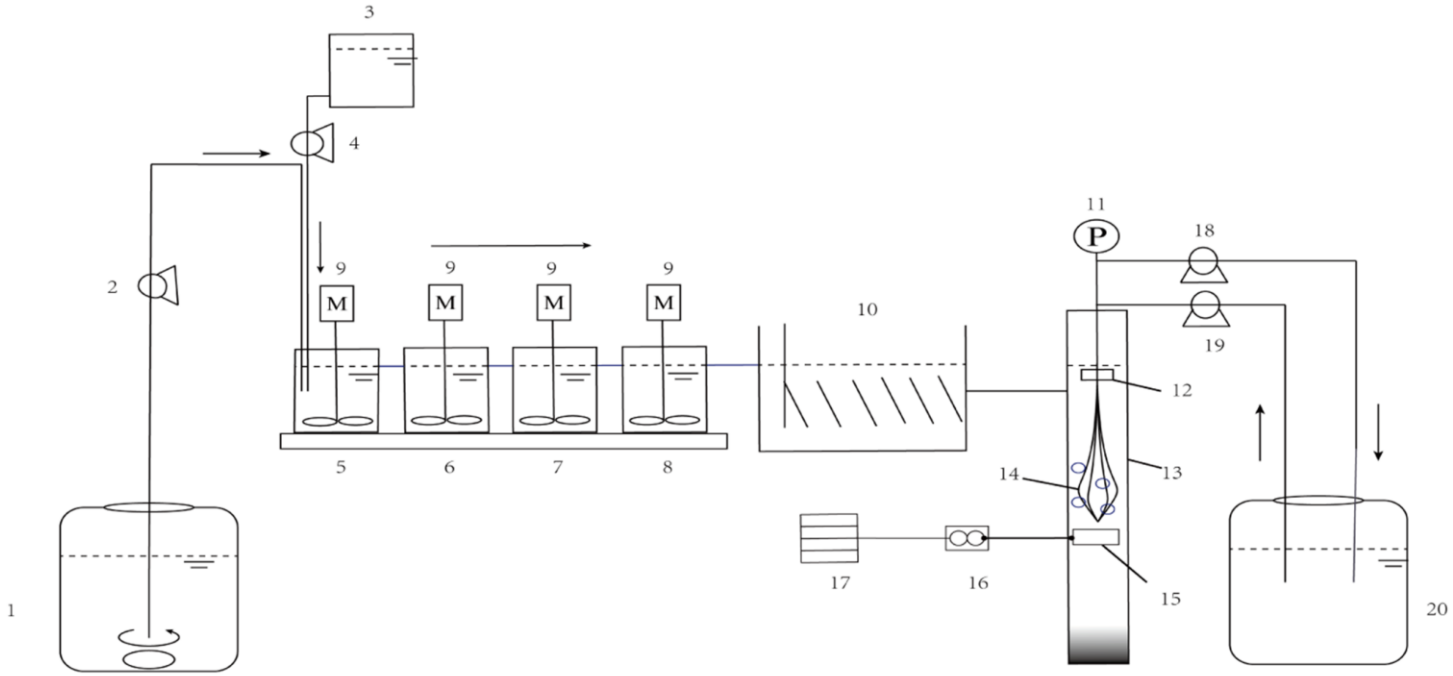

1-raw water tank; 2-feed peristaltic pump; 3-stock flocculation tank; 4-mini peristaltic pump
5-first flocculation tank; 6-second flocculation tank; 7-third flocculation tank; 8-fourth flocculation tank;
9-mechanical stirrer; 10-inclined plate settling tank; 11-pressure gauge; 12-UF membrane module;
13-UF tank; 14-UF membrane; 15-air blower; 16-air flowmeter; 17-air diffuser; 18-suction peristaltic pump;
19-back wash peristaltic pump; 20-produced water tank

Fig. 1. Custom-made continuous-flow flocculation-UF apparatus.

Figure 2

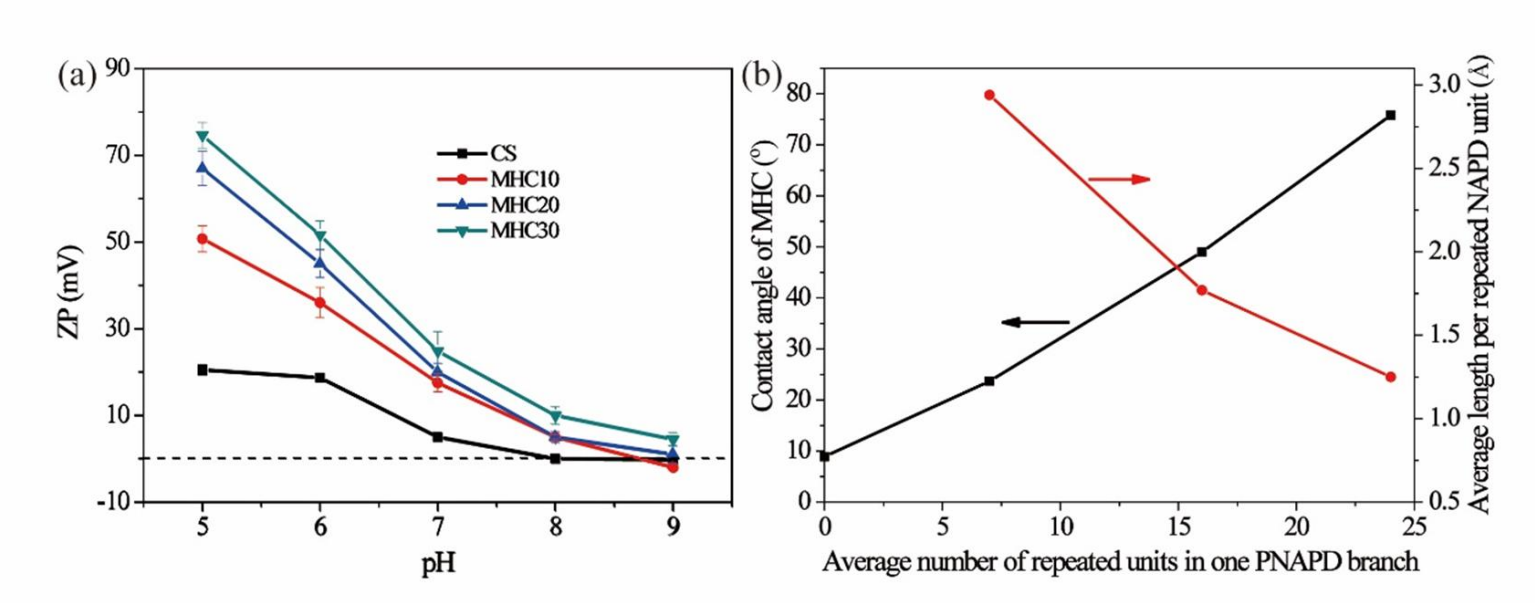

Fig. 2. (a) Zeta potential (ZP) variation with pH for CS and MHCs; (b) Variation of contact angle and average length per repeated NAPD unit of different flocculants (average number of repeated units in one PNAPD branch: MCH10: 7; MHC20: 16; MHC30: 24).

Figure 3

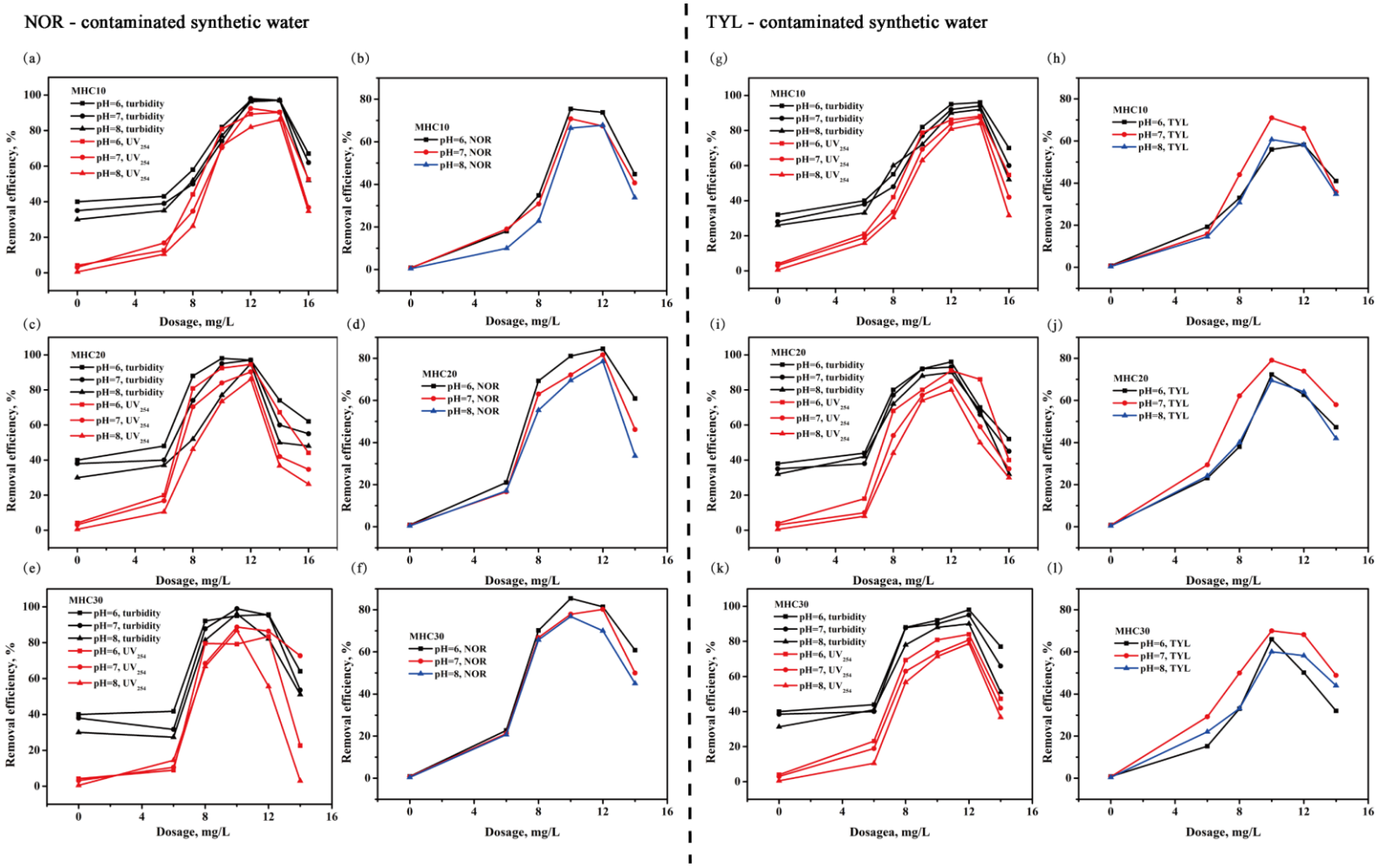

Fig. 3. Performance of MHCs for the treatment of synthetic water in jar flocculation tests.

Figure 4

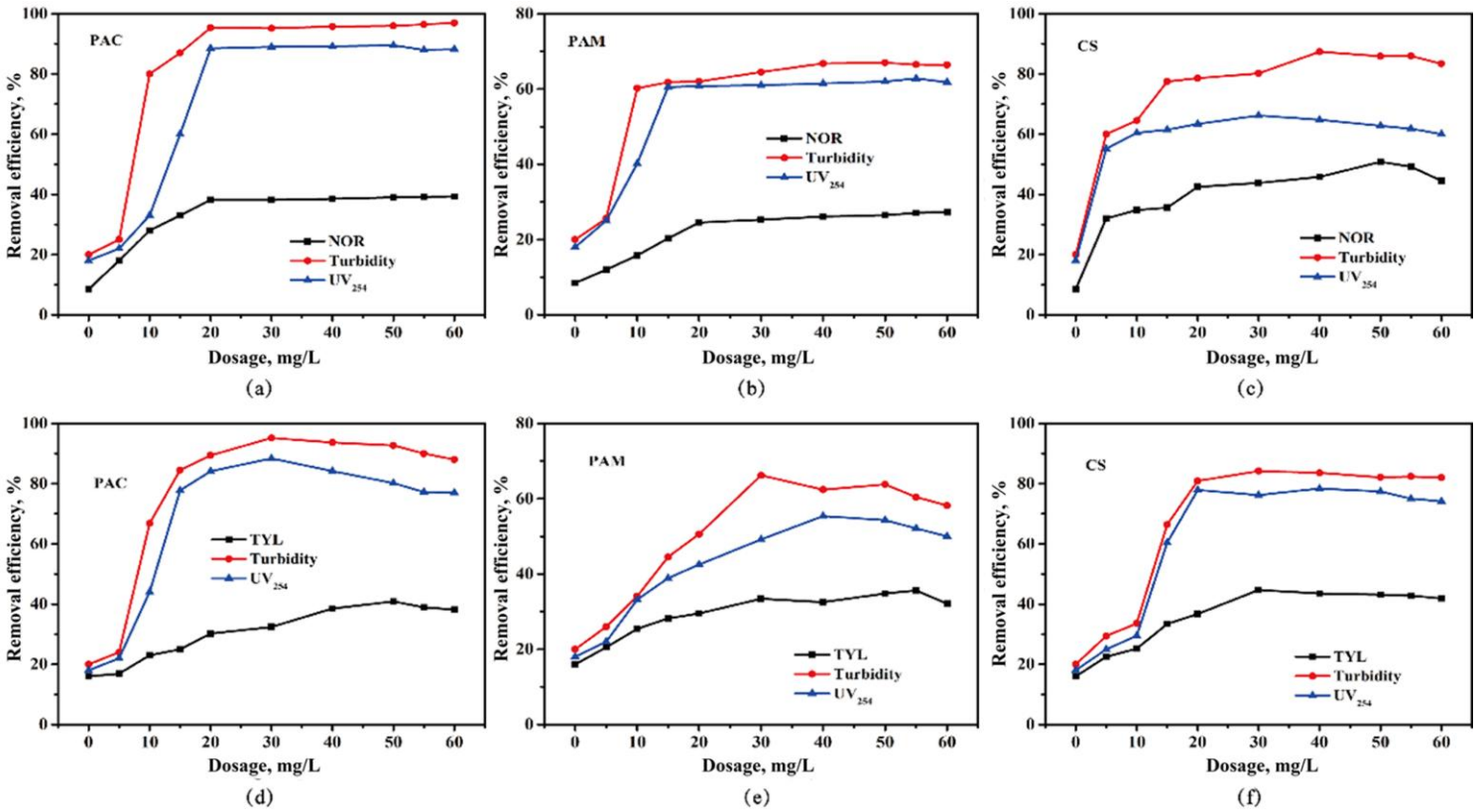

Fig. 4. Flocculation performance of PAC, PAM and CS for treatment of (a-c) NOR- and (d-f) TYL-contaminated synthetic water.

Figure 5

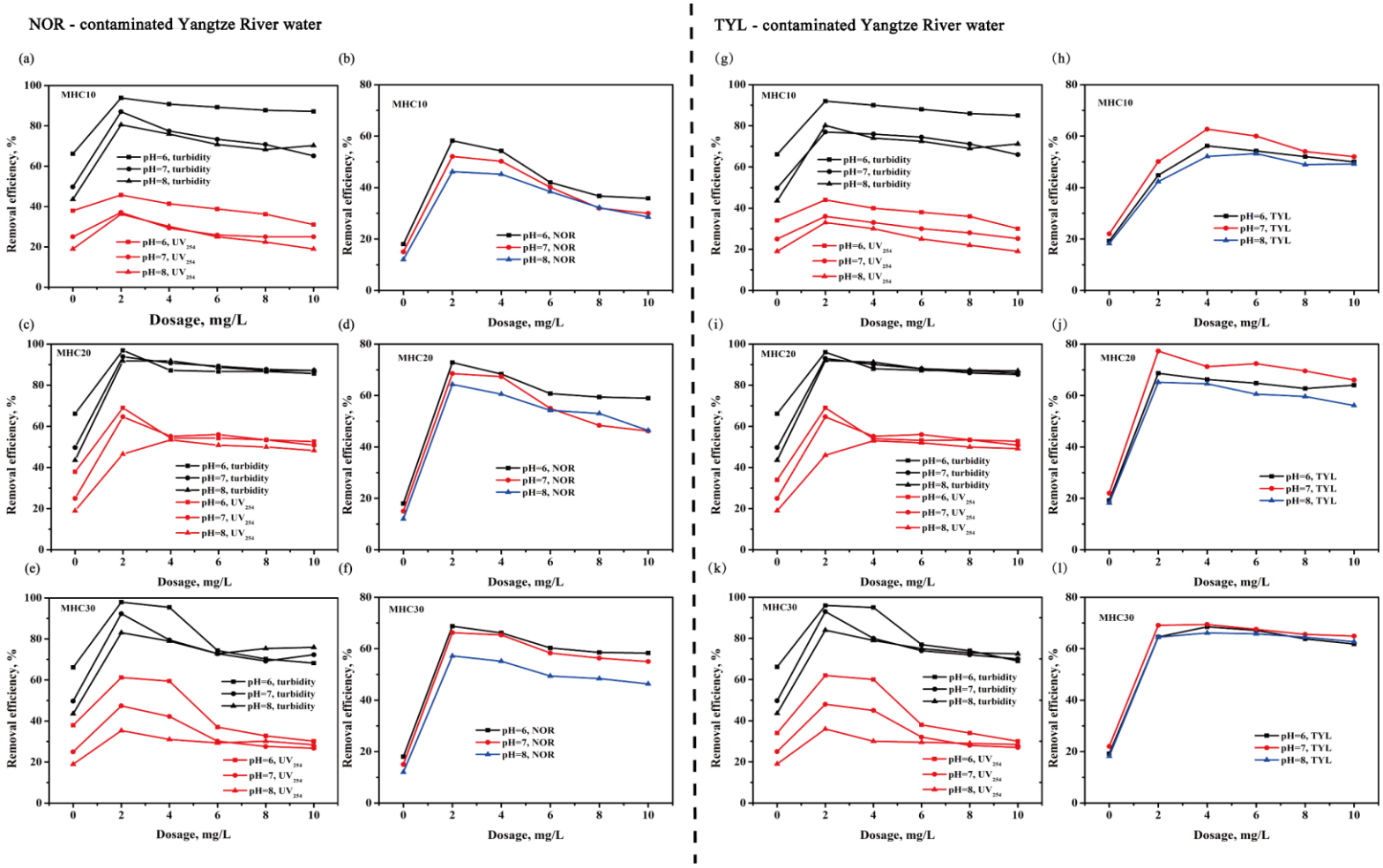

Fig. 5. Performance of MHCs for the treatment of Yangtze River water in jar flocculation tests.

Figure 6

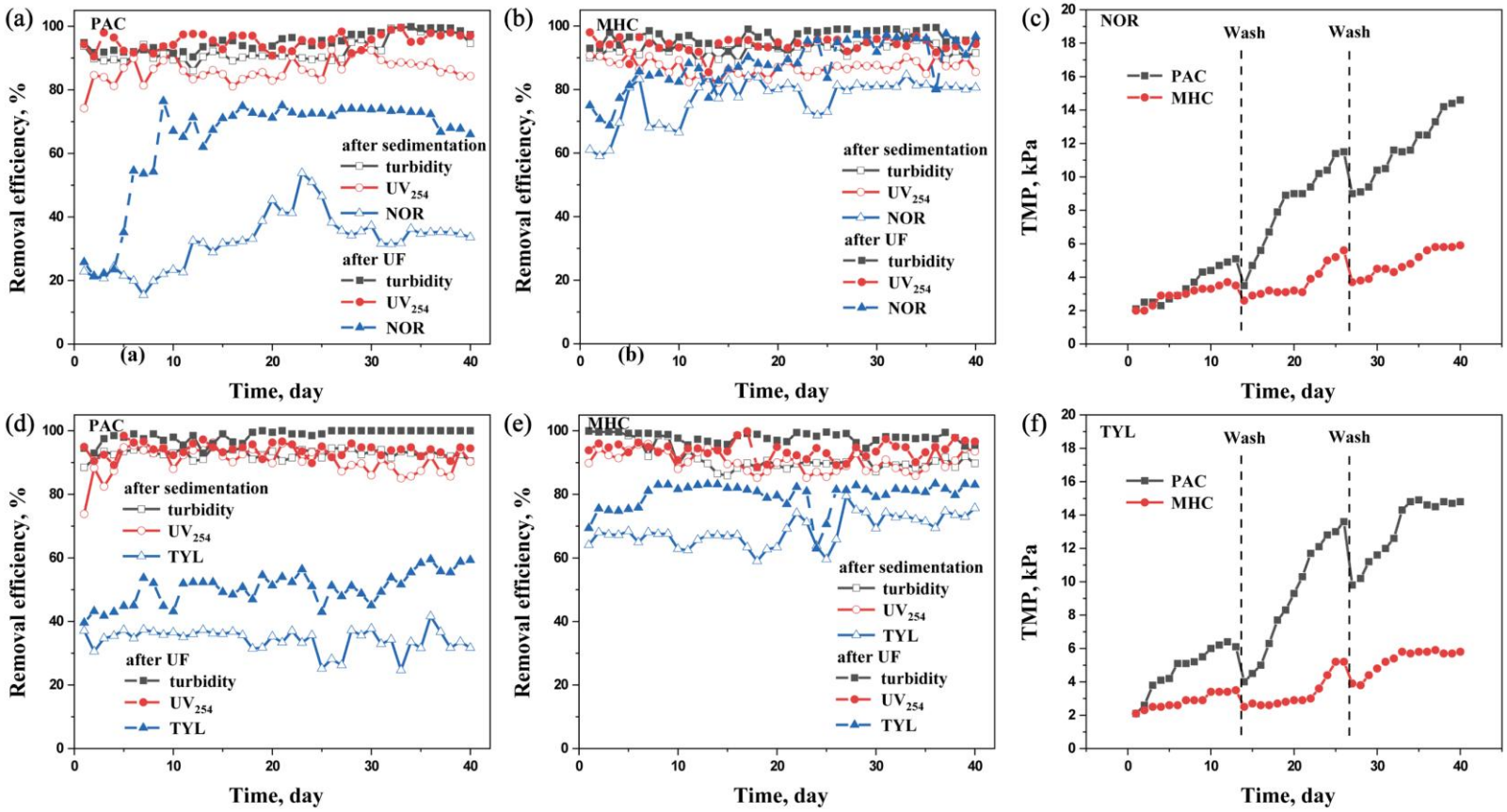

Fig. 6. Performance of MHC20 and PAC for the treatment of (a, b) NOR- and (d, e) TYL-contaminated synthetic water in continuous-flow flocculation-UF tests (water qualities after treatment by (a and d) PAC and (b and e) MHC20; (c and f) variation of TMP with time).

Figure 7

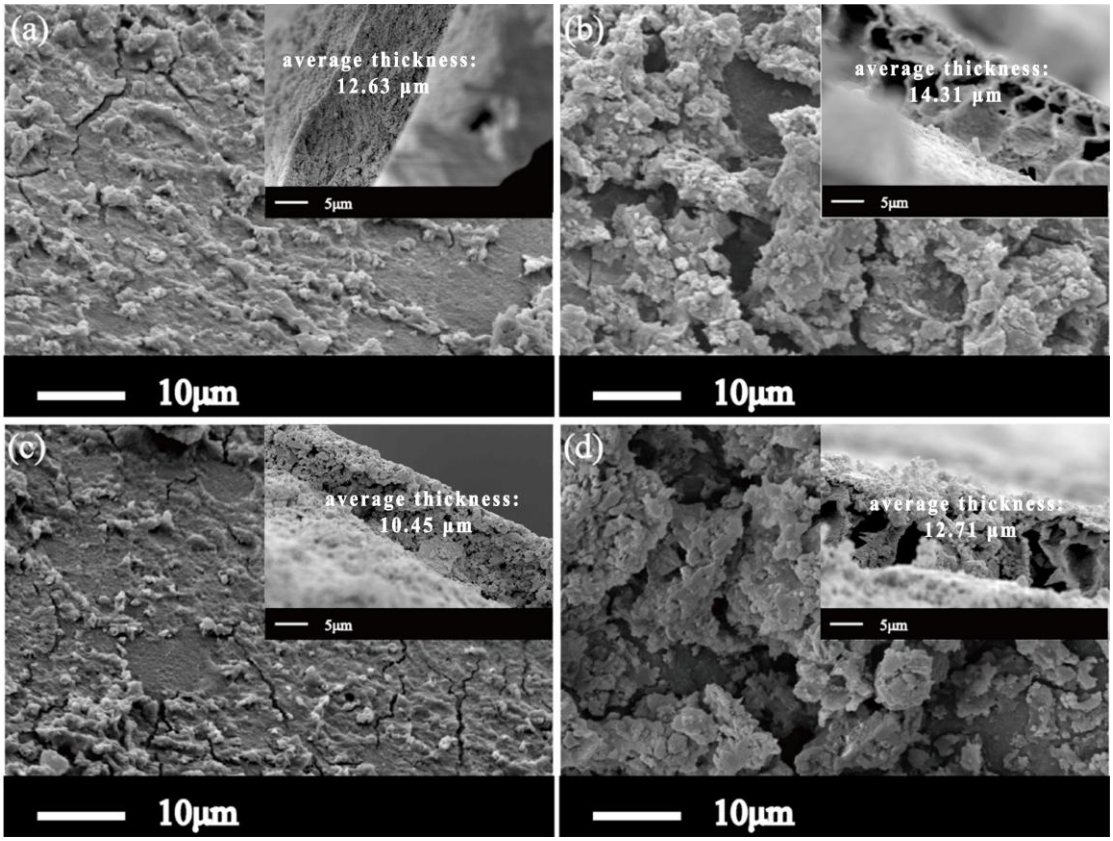

Fig. 7. SEM images of membrane surface after 40 days of flocculation-UF operation for (a and b) NOR- and (c and d) TYL-contaminated water ((a and c) PAC and (b and d) MHC20 were used as flocculants, respectively; Insert figures: Cross-section of cake layers).